SUPPLEMENTAL MATERIAL

Cyclooxygenase-2 in Endothelial and Vascular Smooth Muscle Cells Restrains Atherogenesis in Hyperlipidemic Mice

Soon Yew Tang*, PhD; James Monslow*, PhD; Leslie Todd[#], BS; John Lawson*, MS; Ellen Puré[#], PhD; Garret A. FitzGerald*, MD

From the Institute for Translational Medicine and Therapeutics* Perelman School of Medicine and the Department of Animal Biology[#], School of Veterinary Medicine. Both are at the University of Pennsylvania, Philadelphia, Pennsylvania, 19104-5127.

Address for correspondence: Garret A. FitzGerald, University of Pennsylvania, Perelman School of Medicine, 10-110 Smilow Center for Translational Research, 3400 Civic Center Blvd, Bldg 421, Philadelphia, PA 19104-5158. Email garret@upenn.edu

Supplemental Methods

Preparation of Mouse Aortic Arch and Thoracic Aorta for Real-Time PCR Analysis of Gene Expression

Briefly, mouse aortic tree was perfused with ice-cold PBS dissolved in UltraPure™ DEPC-treated water to minimize degradation of RNA. Mouse aorta was cleaned of adventitial fat and dissected out into aortic arch and thoracic aorta. The aortas were immediately stored separately in RNA*later*® solution (Ambion, Austin, TX) at 4ºC. After 24h, the aortas were transferred to -80ºC for storage until analyses. RNA was extracted using TRIzol® Reagent (Life Tehcnologies, Grand Island, NY) and RNeasy Kit (Qiagen, Valencia, CA) following manufacturer's protocol. Concentration and quality of extracted RNA from aortas were measured using NanoDrop® 1000 (Thermo Scientific, Wilmington, DE) and reverse-transcribed into cDNA using Taqman Reverse Transcription Reagents (Applied Biosystems, Foster City, CA). Quantitative real time PCR was performed using Taqman Gene Expression Assays for Cox-1 (Mm00477214_m1), Cox-2 (Mm00478374_m1), Col1a1 (Mm00801666_g1), and Col1a2 (Mm00483885_m1) using an ABI Prism 7900HT real-time PCR system in a 384 well plate. Results were normalized with GAPDH (Mm99999915_g1).

S. Figure 1

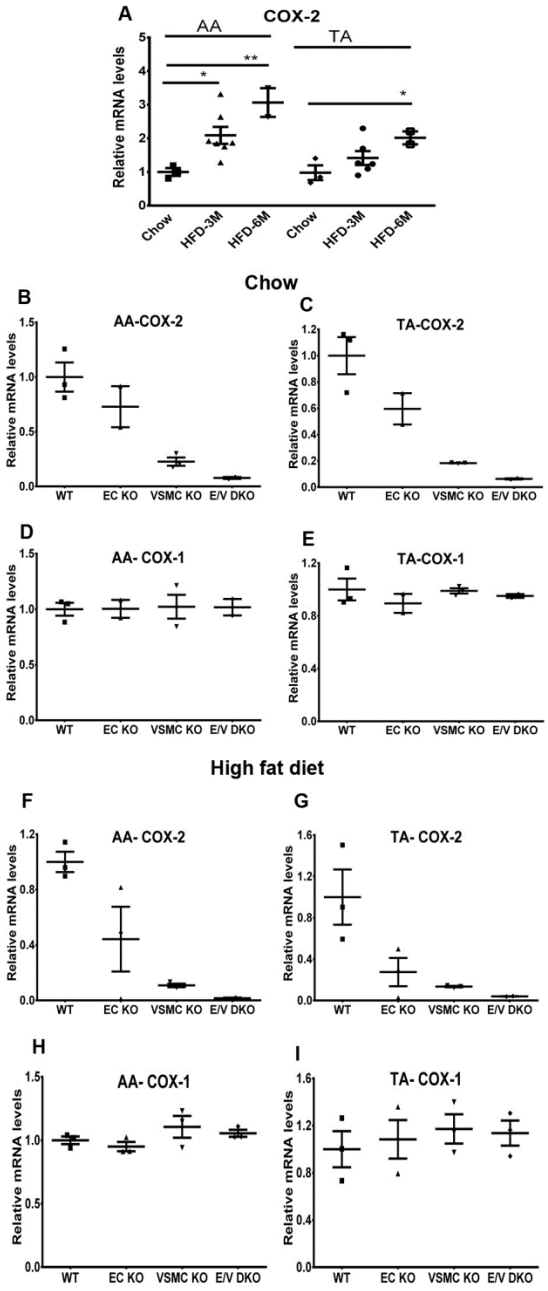
A
COX-2
AA
TA
Relative mRNA levels
Chow
HFD-3M
HFD-6M
Chow
B
AA-COX-2
C
TA-COX-2
D
AA- COX-1
E
TA-COX-1
WT
EC KO
VSMC KO
E/V DKO
High fat diet
F
AA- COX-2
G
TA- COX-2
H
AA- COX-1
I
TA- COX-1

S. Figure 2

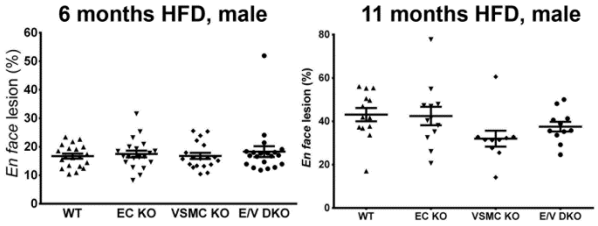
6 months HFD, male
11 months HFD, male
En face lesion (%)
En face lesion (%)
0
10
20
30
40
50
60
0
20
40
60
80
WT
EC KO
VSMC KO
E/V DKO
WT
EC KO
VSMC KO
E/V DKO

S. Figure 3

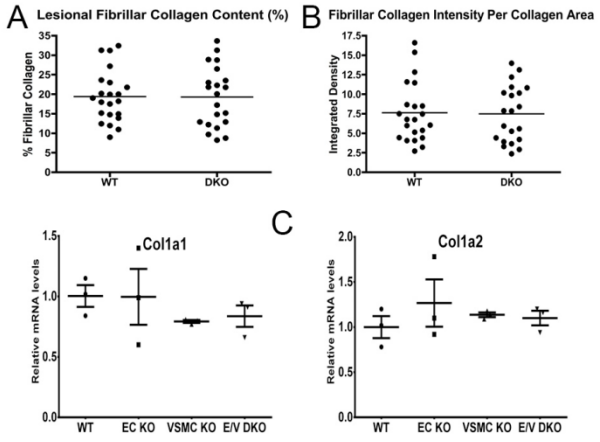
A
Lesional Fibrillar Collagen Content (%)
% Fibrillar Collagen
WT
DKO
B
Fibrillar Collagen Intensity Per Collagen Area
Integrated Density
WT
DKO
C
Col1a1
Relative mRNA levels
WT
EC KO
VSMC KO
E/V DKO
Col1a2
Relative mRNA levels
WT
EC KO
VSMC KO
E/V DKO

S. Figure 4

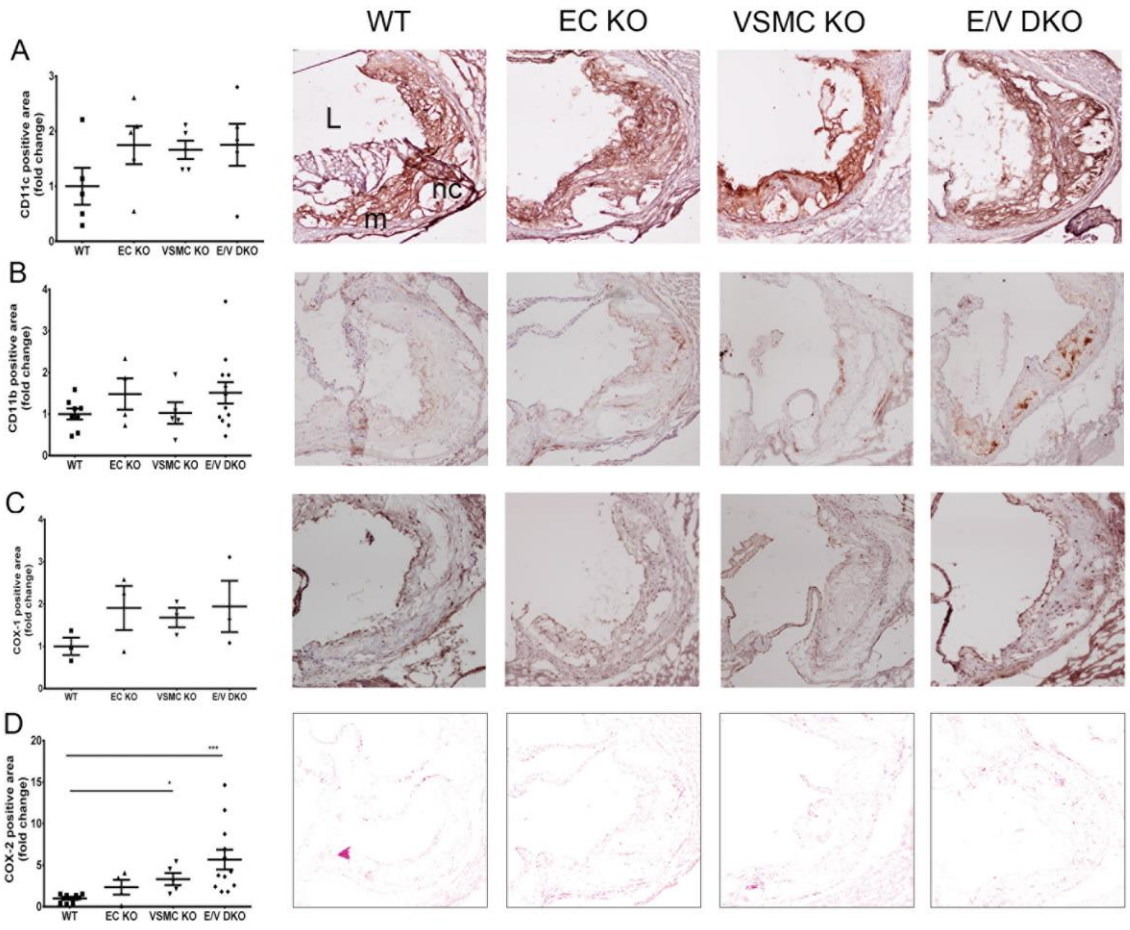
WT
EC KO
VSMC KO
E/V DKO
A
CD11c positive area (fold change)
B
CD11b positive area (fold change)
C
COX-1 positive area (fold change)
D
COX-2 positive area (fold change)
L
nc
m

Supplemental Figure Legends

Supplemental Figure 1. High fat diet up-regulates expression of COX-2 in aortic arch and thoracic aorta. Aortic arch (AA) and thoracic aorta (TA) were dissected and RNA was extracted from WT and COX-2 KO mice on chow (6 months) or HFD (3 and 6 months). COX -2 transcripts were examined by real-time PCR as described in the Methods. A, A trend toward up-regulation of COX-2 in AA and TA after HFD feeding was observed in WT mice. COX-2 mRNA expression levels reflect vascular tissue specific COX-2 deficient mutants both on chow (B and C) or HFD (F and G). The expression levels of COX-1 in AA and TA were minimally altered in WT and COX-2 mutants on chow (D and E) or HFD feeding (H and I). Aortic COX-2 mRNA was increased in mice fed a HFD. Data are means ± SEMs. *$p< 0.05$, **$p< 0.01$, n=2-4 per group.

Supplemental Figure 2. Vascular cell COX-2 fails to modify atherogenesis in male mice after extended periods on a HFD. Aortic atherosclerotic lesion burden, represented by the percentage of lesion area to total aortic area, was quantified by *en face* analysis of aortas from mice fed HFD for 6 or 11 months. One-way ANOVA (Kruskal-Wallis test) showed no significant effects of genotype on lesion progression compared to WT. Data are means ± SEMs. n=18-22 (6 months) or 10-13 (11 months) per genotype.

Supplemental Figure 3. Vascular cell COX-2 deletion has minimal impact on lesional collagen content and intensity, and collagen gene expression in female mice on HFD. A and B, using second harmonic generation two-photon microscopy, quantification of collagen content and intensity were performed in 22 WT and 21 E/V DKO lesions from female mice on a HFD for 6 months. Data are means ± SEMs (Mann-Whitney test, two-tailed, $p> 0.05$). C, Thoracic

aortas were dissected and RNA was extracted from WT and COX-2 KO female mice fed 6 months HFD. Col1a1 and Col1a2 mRNA levels were examined by real-time PCR as described in the Methods. One-way ANOVA (Kruskal-Wallis test) showed no significant effect of genotype on collagen mRNA levels in thoracic aortas of KOs compared to WT, $P > 0.05$. Data are means ± SEMs. n=3 per genotype.

Supplemental Figure 4. Morphometric consequences of vascular COX-2 deletion on lesion development. Lesion morphology in aortic roots from female mice fed 6 months HFD were analyzed. Quantification of immunohistochemical staining of CD11c (A), CD11b (B), COX-1 (C) and COX-2 (D) from WT and KOs are shown in parallel with their representative aortic root sections. One-way ANOVA (Kruskal-Wallis test) showed a significant effect of genotype on lesional COX-2 positive cells ($P=0.01$). Dunnett's multiple comparison tests were used to test significant differences between WT and COX-2 KOs. Despite a trend towards up regulation in staining for CD11c, CD11b, and COX-1 in COX-2 deficient mutants, no significant differences were detected. Data are means ± SEMs. n=3-5 (COX-1 and CD11c), n= 4-12 (CD11b and COX-2). L- lumen, m- media, nc- necrotic core.